COMPARISON OF MSG DENSE ATMOSPHERIC MOTION VECTOR FIELDS PRODUCED BY DIFFERENT METHODS

Szantai A.*, E. Mémin, A. Cuzol**, N. Papadakis**, P. Héas**, B. Wieneke[X], L. Alvarez[+], F. Becker[XX], P.-W. Lopes***

* Laboratoire de Météorologie Dynamique / IPSL, Ecole Polytechnique, 91128 Palaiseau, France
[**] VISTA group, IRISA/INRIA, Campus universitaire de Beaulieu, 35042 Rennes, France
[X] LaVision GmbH, Anna-Vandenhoeck-Ring 19, D-37081 Göttingen, Germany
[XX] University of Mannheim, CVGPR group, D-68131 Mannheim, Germany
[+] AMI group, Universidad de Las Palmas de Gran Canaria, 35017 Las Palmas, Spain

ABSTRACT

This presentation is one of the first intercomparisons between vector fields representing atmospheric motions produced by different methods. Several methods extracting dense motion vector fields based mainly on optical flow techniques have been applied to a dataset of Meteosat Second Generation (MSG) images. The resulting vector fields have then been compared to sparse reference atmospheric vector (AMV) fields calculated with a block-matching (correlation-type) method. Analysed winds are used as complementary data for height assignment or for verification. All the presented methods produce visually consistent vector fields, smoother than the non-dense reference fields. But the high density of vectors is obtained at the cost of losing some outliers (consistent vectors at smaller scales), and having vectors of smaller intensity in average. Differences between results will also be interpreted in relation to the corresponding methods.

1. INTRODUCTION

The derivation of atmospheric motion winds (AMWs) from geostationary satellite images has led to increased wind data coverage of the Earth's surface, and thus has contributed to improve weather forecasts. During the last decade, the quantity (and quality) of AMWs was further increased, due to the arrival of a new generation of geostationary satellites (the new GOES and Meteosat Second Generation - MSG - in particular), with better spatial and temporal resolution of the images and new channels.
To increase again the wind data coverage on the horizontal and on the vertical, other image-processing techniques producing motion vector fields with a denser coverage are taken in consideration. This paper presents and interprets the results of several methods aiming to produce (at least over large areas) dense motion vector fields in 2 dimensions (2D : vectors are on a surface of variable height) and 3 dimensions (3D : a vector fields are determined on a limited number of surfaces corresponding to pressure levels, or pressure ranges). Vector fields are derived from 3 main series of MSG images (reference datasets) corresponding to different meteorological situations and geographic areas. Most techniques are based on the estimation of the optical-flow. Optical-flow estimation methods produce dense motion vector fields. They have been developed since the 1980's, initially for the reconstruction of the motion of solid objects from a pair of images (Horn and Schunck, 1980).

In the next section, the image datasets used for motion vector calculation by the different methods, the atmospheric motion vector (AMV) and wind datasets used as reference will be presented. In section 3, the parameters used to compare two vector files are defined. In section 4, we present briefly the different motion vector calculation methods. The resulting vector fields obtained by the different methods are then compared to the reference wind fields, and differences are interpreted in section 5. General conclusions on methods producing dense vector fields are given in section 6.

This study is part of the European Community project FLUID, dedicated to improve the determination in 2D and 3D of the motion of atmospheric and industrial flows from images. Complementary information on this project can be found on the FLUID website : http://www.fluid.irisa.fr .

2. IMAGE AND MOTION VECTOR OR WIND REFERENCE DATASETS

2.1. Image dataset.

In order to compare motion vector fields for different meteorological situations and geographical areas, three image sets of images have been extracted from full-disk MSG (Meteosat-8) images :

- North-Atlantic + Europe area (NAtl), 5 June 2004, 10:00 – 23:45 UTC ; covers extratropical depressions and a jet-stream. A few pixels in the north-west corner are outside Earth's disk.
- West-Africa + Gulf of Guinea area (AfGG), 5 June 2004, 10:00 - 23:45 UTC ; covers mesoscale convective systems and African monsoon area.
- North-Atlantic + Europe area (NAtl ; same as the first one), 9 Oct. 2005, 0:00 UTC - 10 Oct. 2005, 23:45 UTC ; covers the cyclone Vince, a jet-stream area and an extratropical depression. The Vince cyclone (8-11 October 2005) had a very unusual location. Its trajectory (as a tropical depression) ended over the south-west of Spain.

All images have 1024 x 1024 pixels. Depending on the method, vector fields were derived from a pair or a triplet or a part of the series of images. For all methods, statistics have been determined at 12:00 UTC (on 5 June 2004 and on 9 Oct. 2005) from the vector fields calculated from images in the VIS 0.8 and IR 10.8 channels.

2.2. 2D motion vector reference dataset : LMD AMVs.

Sets of atmospheric motion vectors are calculated with the method developed at the Laboratoire de Météorologie Dynamique (LMD). Its main characteristics are :

- AMVs are calculated with a correlation-type method : the minimisation of the Euclidean Distance, applied on a triplet of images.
- A target (or correlation) window of 12 x 12 pixels and a 12 pixel distance between neighbour gridpoints (smaller than EUMETSAT values) are used.
- Quality tests remove too large or very small or zero vectors. Temporal and spatial symmetry tests are applied in order to retain consistent vectors.
- No direct height assignment is used. The best-fit pressure level is nevertheless derived by comparison with ECMWF analysed winds ; this parameter is used for an independent, qualitative estimation and verification of the height of vectors on 2D fields. It indicates if the vector corresponds to a realistic motion in relation with the clouds observed on the images and the neighbour vectors.

LMD motion vectors were also compared to AMVs produced operationally by EUMETSAT. The latter vectors are calculated with a close algorithm based on the maximisation of the cross-correlation, other parametrisations and a height assignment. Corresponding AMV fields of both datasets appear to be qualitatively consistent.

2.3 3D motion vector reference dataset : ECMWF winds

Analysed winds produced by the ECMWF (European Centre for Medium-range Weather forecast) are available every 6 hours and are used for comparisons with multi-level motion vector fields. As mentioned before, they also give an indicator of the height of the LMD AMVs ; a similar best-fit level parameter can also be calculated for the other 2D vector fields.

3. COMPARISON CRITERIA FOR TWO VECTOR FIELDS

Basically, a 2D vector field is compared to second one used as a reference.

A first element of comparison is the number of motion vectors in each field, or the difference :

$$\Delta NV = NV_1 - NV_{ref}$$

When both vector fields are completely dense, the number of vectors is identical and maximal, and this difference is 0. A different number of vectors can show that a method extracts a different motion. Whatever this number, a method may be more / less efficiently in specific areas, at specific levels, of specific clouds or structures.

3.1 Statistical indicators

For each vector field, the following statistical indicators can be calculated from collocated vectors of two vector fields (the second one is used as the reference field (ref), with N_c common vectors) :

- The bias (in m/s) : $$BIAS = \frac{1}{N_c}\sum_{i=1}^{N_c}\left(V_i - V_{ref\,i}\right)$$
- The RMS vector difference (RMSVD, in m/s) : $$RMSVD = \frac{1}{N_c}\sum_{i=1}^{N_c}\left|\vec{V}_i - \vec{V}_{ref\,i}\right|$$
- The normalised RMS vector difference (NRMSVD, in %) : $$NRMSVD = \frac{RMSVD}{\frac{1}{N_c}\sum_{i=1}^{N_c} V_{ref\,i}} \cdot 100$$
- The angular error (<ΔDIR>, in degrees) : $$\overline{\Delta DIR} = \frac{180}{N\pi}\sum_{i=1}^{N_c}\arccos\left(\frac{\vec{V}_i \bullet \overrightarrow{V_{ref\,i}}}{V_i V_{ref\,i}}\right)$$

3.2 Local comparison of vectors

For each common vector of the reference field, the following coefficients can be calculated :

- the angular difference (in degrees): $$\Delta DIR = \left|angle\left(\vec{V}_1, \overrightarrow{V_{ref}}\right)\right|$$

Values are positive and less than or equal to 180 degrees.

- the relative amplitude of the vector difference (in %): $$R_{vd} = \frac{\left|\vec{V}_1 - \overrightarrow{V_{ref}}\right|}{V_{ref}} \cdot 100$$

Values are positive, between 0 (both vectors are identical) and ∞ (when V_{ref} is zero). In practice, comparisons with a reference vector V_{ref} = 0 are excluded because the comparison coefficients cannot be calculated in that case. When both vectors are identical, the value of both coefficients is 0.

3.3 Comparison of 3D vector fields

Each vector field located at a specific level is compared to the wind fields at the corresponding discrete height(s). In practice, motion vector fields are calculated on 3 ranges of altitude (labelled low, medium and high) and are compared to ECMWF analysed winds fields at discrete levels between 1000 and 700 hPa (for low), at 500 hPa (for medium) and between 400 and 200 hPa (for high) respectively.

4. MOTION VECTOR CALCULATION METHODS

4.1 LaVision method :

The LaVision method used to determine motion vectors from satellite images is a block-matching method based on correlation. It has been initially developed for the tracking of particles in gaseous or liquid flows. It is close in its principle to the LMD method, with some specific elements :

- the spacing between gridpoints (16 pixels) and the target window is larger ;
- the use of multipass calculations, based on an iteration at different scales, starting with a large target window (64 x 64 pixels) ;
- target windows of neighbouring gridpoints partly overlap (75 %) ;
- inconsistent vectors are handled differently (use of a median filter to correct vectors).

4.2 AMI methods : PDE and COR :

The results of two optical-flow methods developed and tested by the AMI group are presented. A description of these methods can be found in a report from the University of Las Palmas de Gran Canaria (Aleman et al., 2005).

- PDE : this method uses partial differential equations for the determination of the motion. The minimisation of a cost function for the optical flow constraint equation enables the determination of the motion vector field. This equation is based on the conservation of intensity and neighbourhood constraints (Nagel-Enkelmann type constraint for regularisation term of optical-flow equation).
- COR : a correlation method is used to estimate the motion : the motion is determined for minimal values of the correlation. A larger target window than the one used in the LMD method has been used.

4.3 VORTEX approach :

VORTEX is a parametric fluid motion estimator based on the detection and tracking of vortices from a series of images, and the use of a stochastic filter. It has been developed by VISTA group (Cuzol and Mémin, 2005). Characteristic structures (vortexes) are extracted on the first images. The association of image data (pixel values on consecutive images), dynamical constraints (Navier-Stokes equation...) and the use of a stochastic filter enable the tracking of these structures on a series of images.
It has been tested on a series of 96 images (24 h) covering a limited area of the Vince tropical cyclone sequence, IR 10.8 channel. It should be noted that the cyclone had a very slow general motion during the test period (9 October).

4.4 ASSIM approach :

Optical flow calculation method based on data assimilation techniques applied on a series of images : the motion vector field is determined when the difference between an “observed" motion vector field (constructed in a first place by an optical flow method) and a predicted motion vector field (calculated from previous fields with equations of dynamics) is minimised. Practically this is expressed by the minimisation of a cost function. Another key element is the “adjoint model", which helps to determine the cost function (or, more precisely, its gradient). A more complete description has been presented on another poster of this conference (Papadakis et al., 2007).
For this comparison, motion vector fields were determined on a series of 117 MSG images of the Vince 2005 cyclone sequences, covering a limited area (256 lines X 512 columns) around the cyclone.

4.5 3D layered motion fields :

A dense motion estimator uses an optical-flow constaint based on the integrated continuity equation and a vorticity- and divergence-based regularisation. Dense motion vector fields are reconstructed on three layers at low-, medium- and high level, including interaction between layers (the vertical motion is also estimated).
Motion vectors are not calculated directly from satellite images, but from pressure difference images, derived from (cloud top) pressure images associated to the cloud classification produced by EUMETSAT (CLA product). A more detailed description of the method can be found in a companion paper (Heas et al., 2007).

5. RESULTS FOR EACH 2D METHOD AND INTERPRETATION

The values of the statistical indicators for the different methods are given in table 1. It should be noticed that these values should be compared with caution, since they correspond to different meteorological situations and geographical areas, and different channels.

Method	**LaVision**	**LaVision**	**AMI COR**	**AMI PDE**	**AMI PDE**	**VORTEX**	**ASSIM**	**ASSIM**
Area	**AfGG**	**AfGG**	**NAtl**	**NAtl**	**NAtl**	**NAtl (red.)**	**NAtl (red.)**	**NAtl (red.)**
Date	**5/6/2004**	**5/6/**	**5/6/**	**5/6/**	**9/10/2005**	**9/10/**	**9/10/**	**9/10/**
Channel	**VIS 0.8**	**IR 10.8**	**VIS 0.8**	**VIS 0.8**	**VIS 0.8**	**IR 10.8**	**VIS 0.8**	**IR 10.8**
$<V_{LMD}>$	7.6	7.8	9.5	9.5	13.2	10.6	11.5	12.
$<V_{meth}>$	7.6	8.1	5.9	8.1	9.6	7.	14.9	14.8
bias	**-0.07**	0.22	***-3.71***	-1.42	***-3.63***	***-3.59***	*3.37*	*2.8*
RMSVD	2.8	3.3	6.5	4.2	8.3	6.8	7.1	5.8
NRMSVD	**36.3**	42.4	***68.4***	43.6	63.1	64.	61.2	48.5
<ΔDIR>	12.7	14.7	***32.1***	14.5	15.5	25.6	13.	**10.7**
NV_{method}	3502	2992	7373	7373	7202	441	903	903
NV_{common}	2239	1852	2888	2888	2060	291	505	505

Table 1 : statistical indicators and number of vectors for the different 2D vector estimation methods. The reference fields are the LMD AMVs. Absolute values close to 0 indicate the greatest resemblance (bold). Largest differences are in *bold italics*. red. stands for reduced area.

For each method, the first figure (*a) represents the reference vector field (LMD AMVs).

5.1 LaVision method (fig. 1b-c) :

From all the vector fields we compared, the LaVision vectors show the greatest similarities to the LMD vectors :
- they cover basically the same parts of the image, once the null-vectors have been removed ;
- most vectors have the same or a close intensity and direction. This is indirectly confirmed by their similar best-fit level.

Some differences can nevertheless be observed :
- the LaVision vector field is smoother ;
- it contains fewer small groups of outliers, i.e. groups with a few vectors that are very different from neighbouring vectors of larger groups. The largest differences between vectors can be observed in areas of high-level clouds or mixed motions (at different levels).
- the LaVision field contains more non-zero-vectors, about 30 % more than the LMD vector field. This is especially true over land (fig. 1b-c). But in the lower part the image, vectors corresponding to (barely visible) low-level clouds are more numerous on the LMD vector field (figure 1a).

Statistical parameters have also been derived from collocated non-zero-vectors (representing 77 % of the LMD vectors and 61 % of the LaVision vectors). LaVision vectors are slightly larger than LMD ones (bias = 0.2 m/s) and the angular vector difference is small (<ΔDIR> = 15°). The normalised RMS vector difference is not negligible (NRMSVD = 42.4 % for an average speed of 7.8 m/s for LMD common vectors) and reflects best the differences between methods.

The LaVision method produces relatively smooth vector fields. This can be explained at least partly by the use of larger and overlapping target windows for the vector calculation, which uses partly common image information and often leads to resembling neighbour vectors : for this case, target windows had a size of 64 x 64 pixels vs. 16 x 16 for LMD, and an overlap of 75 % vs. no overlap for LMD target windows.

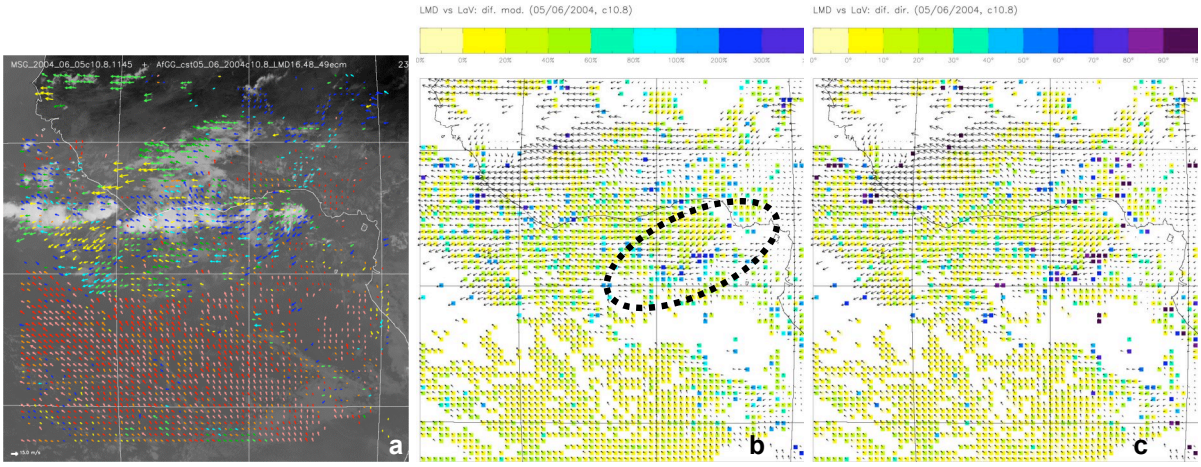

Figure 1 : (a) LMD reference vectors on IR 10.8 image, (b), relative amplitude of vector difference, with superimposed LaVision vectors, (c) angular difference with LaVision vectors. - - - Area of mixed cloud types / important difference in relative vector difference and direction. The best-fit level of LMD vectors is colour-coded : 1000 hPa (pink), 925 (red), 850 (orange), 700 (yellow), 500 and 400 (green), 300 (light blue), 250 and 200 hPa (dark blue).

5.2 AMI PDE method (fig. 2b-c) :

- The COR (cross-correlation) and the PDE methods correctly extract the dominant motion, in particular its direction, but COR's statistical indicators are worse than PDE's when zero vectors are included (figures not shown). Both vector fields are smooth.
- Due to the neighbourhood constraints (regularisation term of the optical flow equation), the motion "spills" over large non-cloudy areas, including the Sahara (figure 2b-c), on the PDE fields. The local comparison of PDE vectors with LMD vectors shows small differences in direction and relative vector difference over a large part of the NAtl area covered by common vectors. The largest differences are found in areas of mixed motion: off the north-western part of the Iberian peninsula and in areas where few clouds are present and tracked by the LMD method (in the western Mediterranean Sea ; centre-right).

- PDE (as well as COR) vectors have in the average a smaller amplitude than LMD AMVs (bias = -1.4 m/s for PDE) . In particular, strong winds are underestimated by PDE-based method.

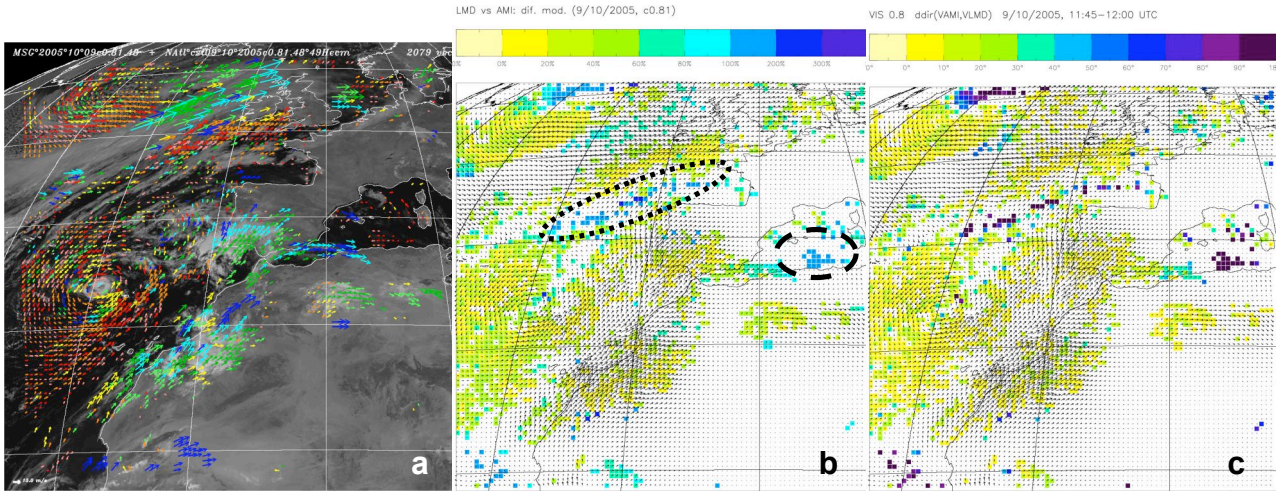

Figure 2 :(a) LMD reference vectors, VIS 0.8 image, (b) relative amplitude of vector difference, and AMI-PDE vectors, (c) angular difference. _ _ _ : small, thin clouds ; - - - - : different motion of clouds at upper / lower level. Same colour-code for best-fit level of LMD vectors as on figure 1a.

5.3 VORTEX method (fig. 3b-c) :

The VORTEX motion vector fields are smooth. They do not either show a fast motion of cloud elements at low-levels found around and in the vicinity of the eye of the cyclone. Nor do they show different motions of clouds at different altitudes, observed on LMD vector field (fig. 3a). VORTEX vectors have a slow (negative) bias.

The position where a null-vector is surrounded by 8 vectors in rotation can be considered approximately as the mathematical centre of the cyclone, since the overall motion of the cyclone at this time (9 October) is very slow. This central position corresponds visually to the position of the eye of the cyclone on the first satellite images.

A different motion of the neighbour cloud at upper right of fig. 3b-c is observed. VORTEX vectors are also larger east of the cyclone centre. Large relative vector differences and difference in direction are possibly due to an edge effect of the algorithm.

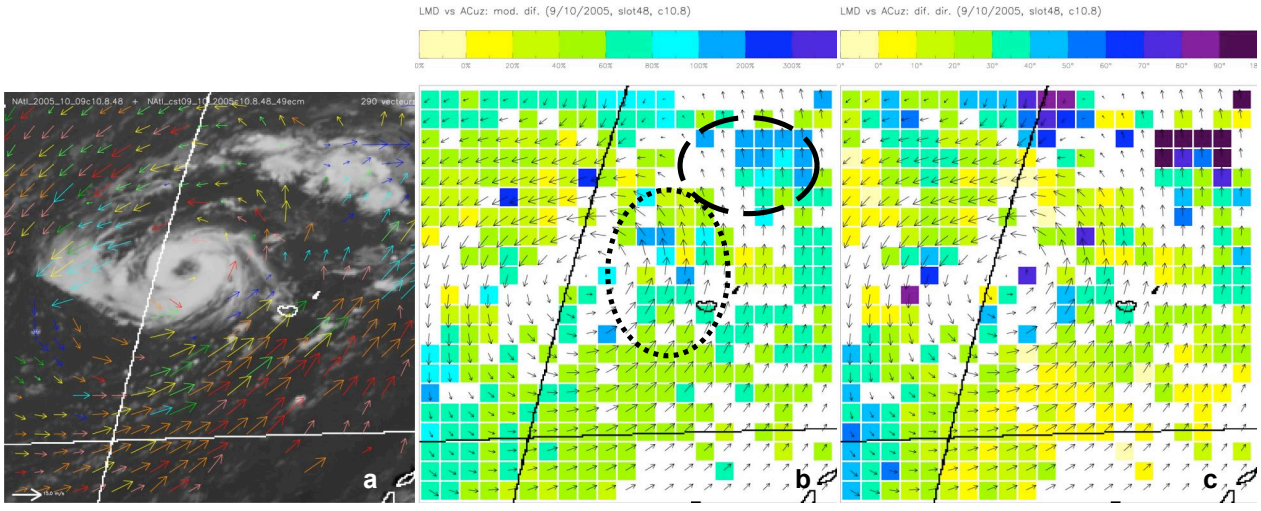

Figure 3 : (a) LMD reference vectors, IR 10.8 image, (b) relative amplitude of vector difference and VORTEX vectors, (c) angular difference. - - - : faster motion on eastern side of cyclone Vince ; _ _ _ : different motion of high-level cloud.

5.4 ASSIM method (fig. 4b-c) :

Figure 4b-c illustrates the rotational motion of clouds around cyclone Vince. The motion vector field is smooth again, as the one calculated by the VORTEX method (fig. 3b-c), with a more realistic restitution of the motion of high-level clouds at the north-east of the cyclone (upper centre of fig. 4 b-c), but still slightly different from the motion observed on the LMD method image (fig. 4a).
Again, the mathematical position of the center of the cyclone is in this example, very close and slightly below the eye of the cyclone visible on the image.

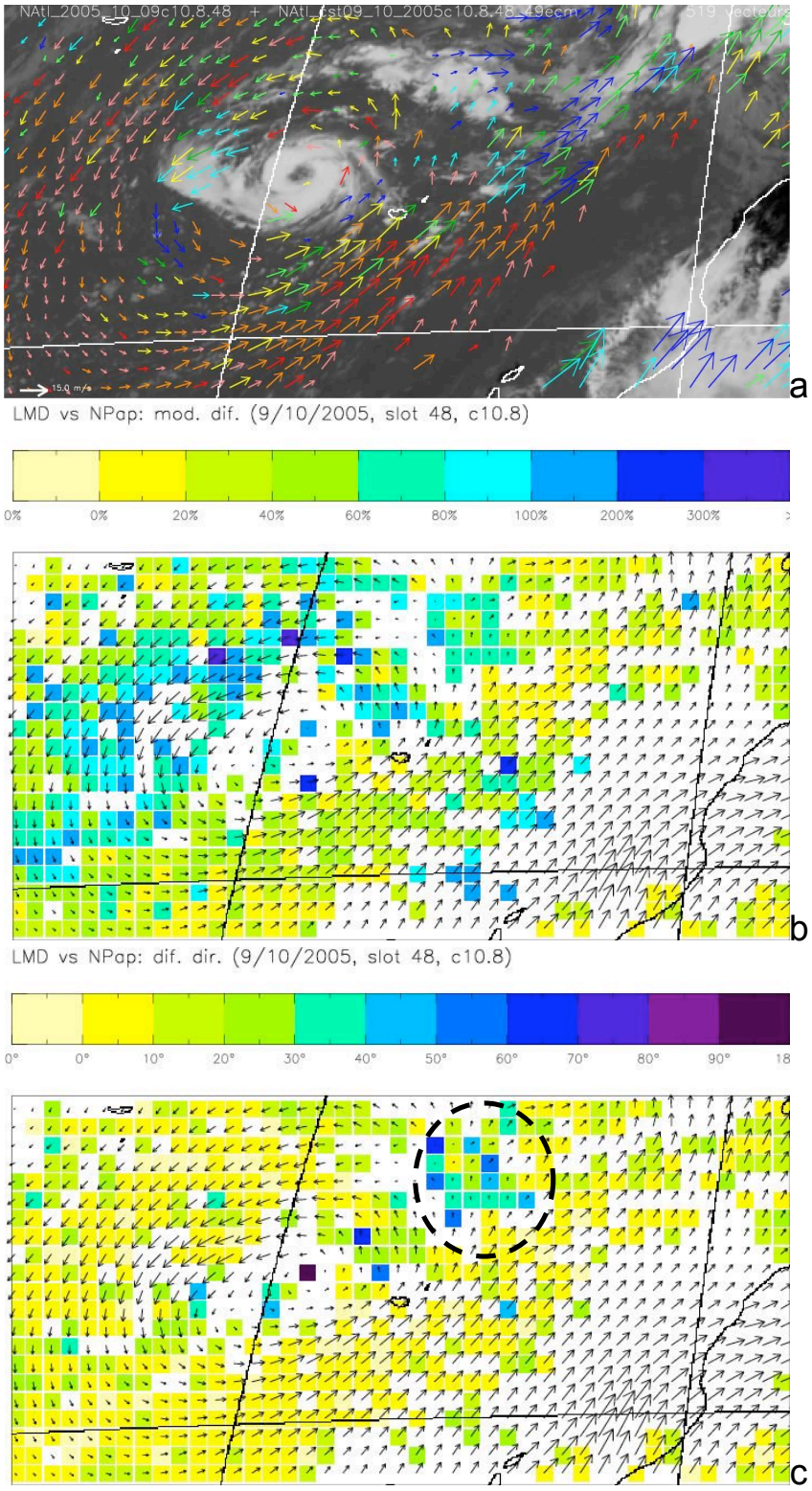

Figure 4 : (a) LMD reference vectors,IR 10.8 image, (b) relative amplitude of vector difference and VORTEX vectors, (c) angular difference. **- - -** : differences of the vectors from the high-level cloud.

The ASSIM method reconstructs the motion more realistically than VORTEX (including non-cyclone clouds). Unlike the other methods, it has a positive bias : ASSIM vectors larger in average than LMD AMVs, except locally close to the centre of the cyclone and on its NE side.

6. CONCLUSIONS

The first conclusion is that all the examined vector fields are smooth. Methods producing dense vector fields have difficulties in tracking different motions in close vicinity or at different levels. A consequence of smoothing is that vectors of all methods except ASSIM are in the average smaller than their LMD counterparts (bias < 0).
The smallest (best) statistical indicators for the LaVision method, closest in its principle to the LMD reference method. A possible explanation for the positive bias observed for the ASSIM method (to be investigated) could be the efficiency of the assimilation process in the method.
All methods extract the dominant motions, but fail to extract small-scale motion, and motions at 2 different levels (not directly measurable at a given position for one channel, but in close neighbourhood).
The results of the 3D layered motion were not satisfactory and are not shown. They only partially recovers motion at the corresponding levels of analysed winds.

Improvements can be expected on all these image-processing methods producing dense vector fields if the following elements are introduced :
- A segmentation of the image based on a cloud classification, and calculation of the motion initially limited to the segments. The resulting motion fields would be dense locally.
- A height determination of the vectors, which can be derived from cloud classification-related products (pressure, height).
- Taking into account the scale of the clouds and structures to track, especially for the correlation-based methods.
The 3D layered motion estimation method is the most promising and should be the closest to real winds, since it includes an image-based motion segmentation (into layers) according to a cloud classification, vertical motion (between layers), and height information (based on pressure), and temporal information (use of a series of images). A reprocessing and verification is under way.

7. BIBLIOGRAPHIC REFERENCES

- ALEMAN, M., L. ALVAREZ, E. GONZALEZ, L. MAZORRA and J. SANCHEZ (2005). Optic flow in fluid images I. Cuadernos del Instituto Universitario de Ciencias y Technologias Cibernéticas, ULPGC, Campus de Tafira, 35015 Las Palmas, Spain. Report 31. 26 p.
- CUZOL, A., E. MEMIN (2005). A stochastic filter for fluid motion tracking. Int. Conf. on Computer Vision (ICCV'05), Beijing, China, Oct. 2005. 7p.
- HEAS, P., K. KRISSIAN, E. MEMIN and A. SZANTAI (2007). Reconstruction and visualization of 3D wind fields from satellite image sequences. Proc. 2007 EUMETSAT Meteorological Satellite Conference – 15th AMS Meteorology and Oceanography Conference, Amsterdam, NL. (24-28 Sept. 2007). This volume, 8 p.
- HORN B. K. P. and B. G. SCHUNCK (1981). Determining optical flow. Artificial Intelligence, **17**, pp. 185-203.
- HEAS P., N. PAPADAKIS, E. MEMIN and A. SZANTAI (2007). Motion estimation of 2D atmospheric layers from satellite image sequences. Proc. 2007 EUMETSAT Meteorological Satellite Conference – 15th AMS Meteorology and Oceanography Conference, Amsterdam, NL. (24-28 Sept. 2007). This volume, 8 p.

8. AKNOWLEDGEMENTS

This study was realised under the European Community contract n° FP6-513663 (Specific Targeted Research Program).